

Article

Cluster Analysis of Freeway Tunnel Length Based on Naturalistic Driving Safety and Comfort

Sen Ma ¹, Jiangbi Hu ^{1,*}, Ershun Ma ², Weicong Li ² and Ronghua Wang ¹ 

¹ Faculty of Architecture, Civil and Transportation Engineering, Beijing University of Technology, Beijing 100124, China; masen@emails.bjut.edu.cn (S.M.); wangrh@bjut.edu.cn (R.W.)

² Shenzhen–Zhongshan Bridge Management Center, Zhongshan 528400, China; maershun@shenzhonglink.com (E.M.); liweicong@shenzhonglink.com (W.L.)

* Correspondence: hujiangbi@bjut.edu.cn; Tel.: +86-(010)-67396181

Abstract: The tunnel is an important component of freeway operation safety, and its classification method is the foundation of a refined management of operation safety. At present, the impact of different categories of tunnels on driver safety, comfort, and driving behavior under naturalistic driving conditions is not clear, and there is a lack of classification methods for tunnels of different lengths in their operation stages. This paper was based on the driving workload, which effectively expresses the safety and comfort of drivers. In this context, naturalistic driving experiments in 13 freeways and 98 tunnels with 36 participants were carried out. The DDTW+K-Means++ algorithm, which is suitable for drivers' driving workload time series data, was used for a clustering analysis of the tunnels. According to the length of the tunnel, the operation-stage tunnels were divided into three categories: short tunnels (<450 m), general tunnels (450~4000 m), and long tunnels (>4000 m). The length of the tunnel had a positive correlation with the drivers' driving workload, while there was a negative correlation with the vehicle running speed, and the range of changes in the drivers' driving workload and operation safety risks in general tunnels and long tunnels was higher than that in short tunnels. Road and environmental conditions are important factors affecting the driving workload. The entrance area, the exit area of tunnels, and the middle area of long tunnels are high-risk sections in the affected area of the tunnel. These research results are of great significance for the operation safety management of freeway tunnels.



Citation: Ma, S.; Hu, J.; Ma, E.; Li, W.; Wang, R. Cluster Analysis of Freeway Tunnel Length Based on Naturalistic Driving Safety and Comfort. *Sustainability* **2023**, *15*, 11914. <https://doi.org/10.3390/su151511914>

Academic Editor: Matjaž Šraml

Received: 10 July 2023

Revised: 27 July 2023

Accepted: 31 July 2023

Published: 2 August 2023



Copyright: © 2023 by the authors. Licensee MDPI, Basel, Switzerland. This article is an open access article distributed under the terms and conditions of the Creative Commons Attribution (CC BY) license (<https://creativecommons.org/licenses/by/4.0/>).

Keywords: tunnel length; tunnel classification; driving workload; naturalistic driving experiment

1. Introduction

With the rapid development of the economy, the mileage of freeways has rapidly increased. Tunnels possess many advantages, such as improving linear standards, shortening driving mileage, and protecting the ecological environment, and their proportion in freeways has also rapidly increased. The tunnel is relatively closed, with significant changes in road and environmental conditions, and the driving behavior is different from standard freeway sections, which can easily lead to traffic congestion and can increase traffic safety risks [1,2]. Once an accident occurs in a tunnel, it easily results in a secondary accident, and the severity of the accident and property damage are higher in tunnels than in standard freeway sections [3–5]; thus, the traffic danger situation can be more severe.

There are many causes of tunnel accidents and many factors influencing traffic safety [6–8]; human factors account for more than 85% of the factors [9], and they are also the core cause of tunnel accidents. The impact of other factors in the traffic system, such as vehicles, roads, and the environment, will also be reflected in driver psychology and driving behavior. Drivers driving vehicles from the standard freeway section into the affected area of the tunnel, in turn, drive through the preview area, entrance area, middle area, exit area, and separation area. The road headroom, cross-section, lighting

environment, landscape, etc., are constantly changing, stimulating drivers to varying degrees [10,11], thus causing changes in drivers' psychophysiological states. This can affect driving safety, comfort, and behavior, which—in turn—affects tunnel traffic safety [12–15]. The length and traffic safety facilities of tunnels can also have different impacts on the psychophysiological characteristics and driving behavior of drivers. Therefore, clarifying the impact of tunnel length on the psychophysiological indicators of drivers and classifying tunnels based on length are the foundation for a more-refined management of tunnels and for ensuring traffic safety in tunnels.

Tunnel traffic safety and the psychophysiological and behavioral characteristics of drivers have attracted the attention of many scholars. Calvi et al. studied the traffic characteristics of the different sites of a tunnel using driving simulation and proposed a method for evaluating the length of tunnel entrance and exit areas [16,17]. Wang et al. investigated the effect of the entrance and exit area on extra-long tunnel safety by recording driver eye-movement parameters; the research results indicated that there were significant differences in the visual load of drivers in different areas and times of the tunnel [18]. Feng et al. used heart rate growth (HRG) to analyze the psychological changes that occur in drivers when driving through a tunnel, as well as established a model of the relationship between HRG, speed, and longitudinal grade. Furthermore, they studied the effect of longitudinal grade on HRG and speed and proposed that the psychological tension of drivers is higher when driving downhill in a tunnel [19]. Yang et al. analyzed vehicle speed and drivers' electroencephalography characteristics in the tunnels via a naturalistic driving experiment, which indicated that the drivers' electroencephalography power change rate in the upslope area of tunnels is higher and has the greatest impact on driving safety [20]. Rendon-Velez et al. used driving simulation to study drivers' psychological and driving behavior characteristics in tunnels. Moreover, when the driving tasks were different, there were significant differences in the drivers' psychological parameters (eye-movement parameters, heart rate, respiratory rate, etc.) and driving behavior characteristics (vehicle running speed, braking, throttle, etc.) [21]. Qi et al. analyzed the pupil diameter and heart rate (HR) variation pattern of drivers when driving in tunnels via driving simulation, and they proposed corresponding fitting functions to study the driving load. Furthermore, they proposed a classification method for tunnel risk levels and established a fusion model based on the average pupil diameter and heart rate growth functions, but they did not consider the effects of different categories of tunnels on drivers [22]. At present, researchers mostly use driving simulations for drivers' psychological characteristics and driving behavior in tunnels studies [23]. However, driving simulations are less realistic than naturalistic driving experiments where vehicles or drivers are equipped with testing equipment to collect data on normally traveled roads [24]. Therefore, the results obtained using driving simulation are not as reliable as naturalistic driving.

In terms of tunnel classification, Fu et al. analyzed the differences in driving behavior and visual perception for short, medium, and long tunnel entrance areas under a naturalistic driving approach. However, the classification was based only on design specifications, and Fu et al. did not study the classification method for the operation stages of the tunnel [25]. Amundsen, Guillermo, and Ma et al. classified tunnels into 3~5 categories based on length when studying tunnel safety and accident characteristics, but they did not provide specific classification criteria [4,5,9]. In the Netherlands, tunnels are classified into short and long tunnels according to their lighting conditions and whether there is a "black hole" phenomenon at the tunnel entrance. Norway, Japan, the United Kingdom, China, and the United States classify tunnels into 3~6 categories, mainly based on tunnel length, traffic volume, traffic density, traffic composition, and the cross-sectional types of tunnel openings [26–29]. Chen et al. established a tunnel management classification discriminant function by considering the safety correction coefficients for tunnel importance, civil construction characteristics, traffic characteristics, and operation management characteristics; they determined the tunnel category according to the threshold interval to which the calculated value of the discriminant

function belongs, thus classifying tunnels into three categories [30]. However, the current research and design specifications for tunnel classification do not consider driving safety, comfort, and behavior from a driver's perspective, thus resulting in the existence of many difficulties in tunnel operation and management.

Compared to the standard freeway section, the conditions of the road, traffic, and environment in the affected area of the tunnel change drastically. The stimulation of drivers in the affected area of the tunnel is different from that of other road sections; the physiological and psychological changes that drivers experience during driving in the affected area of the tunnel are the driving workload [31]. Different tunnel lengths will have different impacts on drivers; at present, the impact of different categories of tunnels on driver safety, comfort, and driving behavior under naturalistic driving conditions is not clear. Thus, there is a lack of classification methods for tunnels of different lengths during the operation stages. In order to analyze the impact of different categories of tunnels on driver safety, comfort, and driving behavior, naturalistic driving experiments under different lengths of tunnels were conducted, and a tunnel length classification method is proposed in this paper. The research results are of great significance for reducing the accident rate and severity of accidents in tunnels and ensuring the safety of tunnel usage.

2. Methodology

Rapid changes in road, traffic, and light environmental conditions in the affected area of the tunnel will stimulate drivers to varying degrees, and this determines the drivers' driving workload. The drivers' ability is limited and can only process 3–4 pieces of information simultaneously. Excessive or insufficient information can lead to poor driving workload, which in turn affects driving behavior and is highly correlated with traffic accidents. Complex road and traffic conditions, as well as excessive traffic sign information can provide drivers with excessive stimulation, resulting in a higher driving workload and reducing their perception and processing ability of information, as well as increasing the risk of dangerous driving behavior. On the contrary, this can lead to a lower driving workload, which can easily lead to driving fatigue and improper handling of emergency situations. At present, the driving workload has been widely applied in the evaluation and research of road safety.

In recent years, with the development of medical and wearable detection devices, scholars have continuously explored the relationship between the psychological characteristics of road users and traffic safety [32]. Heart rate variability (HRV) is an indicator that measures changes in the time interval between heartbeats and is related to human psychological phenomena, mainly including time domain and frequency domain indicators. The low-frequency (*LF*) power in the frequency domain index is related to the activity of the sympathetic nervous system; the high-frequency (*HF*) power is related to the activity of the parasympathetic nervous system, and their ratio (*LF/HF*) reflects the balance of the parasympathetic nervous system and sympathetic nervous system activities. It is reliable and easy to measure, and it can be adopted to measure the driving workload. When drivers are stressed or fatigued, their heart rate will change; the HRV index can characterize the change in heartbeat cycle variability, which, in turn, reflects a driver's driving stress and fatigue [31,33]. The measurement model of the driving workload is shown in Equation (1):

$$K_{ij} = [(\frac{LF}{HF})_{ij} - A_i] / V_{ij} \quad (1)$$

where K_{ij} is the driving workload of driver i at position j ; LF is the low-frequency power; HF is the high-frequency power; $(LF/HF)_{ij}$ is the HRV of driver i at position j ; A_i is the HRV when driver i is driving normally; and V_{ij} is the running speed when driver i is at position j , in km/h.

The classification thresholds for a driving workload are shown in Table 1 [31].

Table 1. Threshold values for the safety classification of driving workload on a freeway.

Driving Workload Degree	Safety Level	Driving Workload
Highest	Highly risky (nervous)	$K_{ij} > 0.060$
Higher	Relatively risky (relatively nervous)	$0.030 < K_{ij} \leq 0.060$
Normal	Safe	$-0.001 < K_{ij} \leq 0.030$
Lower	Relatively risky (relatively fatigued)	$-0.012 < K_{ij} \leq -0.001$
Lowest	Highly risky (fatigue)	$K_{ij} \leq -0.012$

3. Experiment

3.1. Participants and Vehicles

The different characteristics of the drivers will have a significant impact on the naturalistic driving experiment. A total of 36 participants with good physical conditions and no history of cardiovascular disease or of heart disease were randomly recruited. The participants had experience driving on freeways, had no major accidents, were not familiar with the experiment road and tunnel, and had normal vision or corrected vision. There were no behaviors such as drinking alcohol or staying up late 72 h before the start of the experiment, and no excitatory substances such as caffeine and nicotine were consumed 3 h before the start of the experiment. The 36 participants, including 25 men and 11 women, met the gender ratio of Chinese drivers. The age of the participants was 21~58 years ($M = 36.9$, $SD = 9.9$). The driving experience range of the participants was 2~31 years ($M = 11.3$, $SD = 8.1$). The annual average driving mileage of the participants was 2000~15,000 km ($M = 6108$, $SD = 3284.3$).

Representative cars running on the freeway were used as the experimental vehicles.

3.2. Instruments and Equipment

A physiological detector was used to collect the participant's HRV data, with a continuous working time > 24 h, and error < 3 times/min, with a sampling frequency of 60 Hz; the physiological detector did not affect the participant's normal driving.

A Dynamic GPS was used to determine vehicle position, with an error < 3 times/min, sampling frequency of 10 Hz, and resolution < 0.03 m/s.

A non-contact multifunctional speedometer was used to collect the running speed and distance of the vehicles in the tunnel, and it was also used to calibrate the characteristic positions inside the tunnel, with a sampling frequency of 60 Hz, a speed range of 0~250.00 km/h, a resolution of 0.01 km/h, and a distance range of 0~99,999.999 m, with the resolution in 1 mm.

The instruments and equipment are shown in Figure 1.

3.3. Experiment Road and Tunnel

Thirteen typical four-lane freeways with normal traffic in China were selected for the experiment, and the speed limit was 80 km/h. The experimental road included a total of 98 bidirectional double-hole independent tunnels; there were no other tunnels within 3 km of the experimental tunnel; the length of the tunnel was 54~12,330 m. The conditions of the experiment road and tunnel met the requirements of current Chinese regulations, ensuring that the road alignment conditions did not affect the driving workload. The lighting, ventilation, and traffic safety facilities of the experiment road and tunnel were set up in accordance with the current Chinese standard. Except for the standard freeway section (S), the affected area of the tunnel mainly included the following sites (shorter tunnels only included some sites), as shown in Figure 2:

- (1) Preview area (A): This area is the section where the driver is 200 m before the tunnel information sign to when he/she is one stopping sight distance from the tunnel entrance. This section extended from 500 m before the tunnel entrance to 110 m before the tunnel entrance.

- (2) Entrance area (B): This area is the section where the driver is one stopping sight distance before the tunnel entrance to him/her entering the tunnel (i.e., where the tunnel lighting environment no longer changes). This section extended from 110 m before the tunnel entrance to 200 m after the tunnel entrance.
- (3) Middle area (C): This area is the section of the tunnel where the lighting environment does not change. This section extended from 200 m after the tunnel entrance to 200 m before the tunnel exit.
- (4) Exit area (D): This area is the section where the lighting environment begins to change to where the driver is one stopping sight distance after the tunnel exit. This section extended to 200 m before the tunnel exit to 110 m after the tunnel exit.
- (5) Separation area (E): This area is the section where the driver is one stopping sight distance after the tunnel exit to when the tunnel no longer impacts the driver. This section extended from 110 m after the tunnel exit to 500 m after the tunnel exit.



Figure 1. Instruments and equipment used in the experiment. (a) Physiological detector; (b) Dynamic GPS; (c) non-contact multifunctional speedometer.

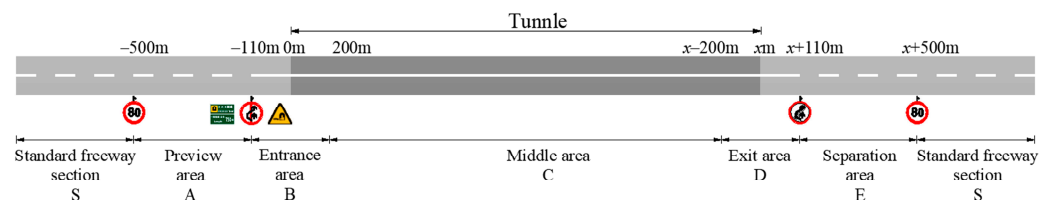


Figure 2. Schematic diagram of experimental roads, tunnels, and facility settings.

3.4. Experimental Procedures

The experiment was conducted from March to May (when the weather was good), 8:00~12:00 and 14:00~18:00, 36 days in total. The main experimental procedures were as follows:

- (1) Provide unified training for participants; inform them of the precautions for experiment, and familiarize them with the experimental vehicle.

- (2) Install instruments and equipment for vehicles and participants; adjust the instruments and equipment to normal working conditions, and maintain consistency in the timing of the instruments and equipment.
- (3) The participant sits quietly in the car for 5 min to collect the participant's resting physiological data.
- (4) The participant drives the vehicle through the experiment road and tunnel normally.

To eliminate the effect of other conditions on the experiment results, during the experiment, it should be ensured that the traffic conditions are free-flow ($k < 7$ veh/km·ln); a single test section did not exceed 40 km; the participants were not informed in advance of the conditions for the experiment road and tunnel. During the experiment, a recorder was assigned to record the time when the participant passed an important point and the participant's behaviors. After driving on a single test section, the participant's subjective feelings about each tunnel was recorded; after the participant driver completed all test sections, the number of tunnel classifications based on the participant's subjective driving experience was also recorded. After the experiment, each participant was paid for his/her participation. All ethical standards during the experiment were adhered to.

3.5. Data Analysis

In this paper, MATLAB and SPSS were used to process and analyze the data. After removing the abnormal data caused by the abnormal driving behaviors of the participants and due to collection equipment failures, the experiment yielded—for 36 participants under 98 tunnels—a total of 2,051,267 pieces of HRV physiological data, 1,675,612 pieces of vehicle GPS data, and 2,078,741 pieces of non-contact multifunctional speedometer data.

4. Cluster Analysis of Tunnel Length

4.1. Subjective Evaluation of Participants

The subjective ratings of the participants were collated, and the results are shown in Table 2. A total of 48.1% of the tunnels made participants feel only nervous while driving. Fewer tunnels made participants feel not nervous and not fatigued (28.2%) or both nervous and fatigued (20.1%), while only 3.6% of the tunnels made participants feel only fatigued. Regarding the number of tunnel categories, the majority of participants (69.4%) believed that the tunnels should be classified into three categories according to their driving experience. A minority of participants (19.5%) believed that they should be classified into 4 categories, and the remaining (albeit especially few) participants believed that they should be classified into 2 or 5 categories. Therefore, depending on the subjective driving experience of most participants, tunnels should be classified into 3 or 4 categories.

Table 2. The subjective evaluation results of the participants.

Participants Status	Not Nervous and Not Fatigued	Only Nervous	Only Fatigued	Nervous and Fatigued
Participant Proportion	28.2%	48.1%	3.6%	20.1%
Number of Tunnel Classifications	2	3	4	5
Participant Proportion	2.8%	69.4%	19.5%	8.3%

4.2. Clustering Algorithm

4.2.1. Euclidean Distance and the K-Means Algorithm

Clustering is a process of aggregating samples by similarity (distance), i.e., clustering similar (or close) samples into the same category and dissimilar (or distant) samples into other categories.

The different tunnels and driving workload of the participants constituted a time series of different "length" and "shape", and the Euclidean distance is usually used to

calculate the distance between these two time series. For the time series $x = (x_1, \dots, x_m)$ and $y = (y_1, \dots, y_m)$, the Euclidean distance ED between them is shown in Equation (2):

$$ED(x, y) = \sqrt{\sum_{i=1}^m (x_i - y_i)^2} \quad (2)$$

K-Means is a common clustering algorithm; K data samples are randomly selected as the initial centers of K clusters, and the remaining data samples are assigned to the closest cluster according to their distance from each cluster center. The mean value of the data samples in each cluster is then recalculated, and the result is used as the new cluster center. Next, the above steps are repeated until the objective function converges. The data are then finally clustered into K categories, and the objective function is shown in Equation (3) [34]:

$$\min \sum_{i=1}^k \sum_{x_i \in C_i} dist(C_i, x_i)^2 \quad (3)$$

where C_i is the set containing samples in category i ; $dist(C_i, x_i)$ is the distance between C_i and x_i .

K-Means is a conventional unsupervised clustering algorithm. Due to the different lengths of tunnels and vehicle running speeds, the “length” and “shape” of the time series formed by the driving workload in the experiment were different. A clustering algorithm that is based on a one-to-one Euclidean distance is difficult to use in effectively identifying the similar curve patterns under different “lengths” and in curves with similar distances, but large differences in “shape”.

4.2.2. K-Shape Algorithm

To identify the different “shapes” of the time series, the K-Shape clustering algorithm, which preserves the shape of the time series, can be used. The K-Shape algorithm uses the normalized cross-correlation coefficient ($NCCc$) as a distance measure, calculates the cluster centroid, uses one time series to characterize a set of time series, and extracts data samples with a representative “shape” to cluster the time series. The K-Shape algorithm consists of the following steps [35]:

(1) Shape-based distance (SBD):

For the time series $x = (x_1, \dots, x_m)$ and $y = (y_1, \dots, y_m)$, their similarity is shown in Equation (4):

$$CC_w(x, y) = R_{w-m}(x, y) \quad w \in \{1, 2, \dots, 2m-1\} \quad (4)$$

where $CC_w(x, y)$ is a mutual correlation sequence of length $2m-1$; R is the sum of the dot products of the effective regions; $R_{w-m}(x, y)$ is shown in Equation (5):

$$R_{w-m}(x, y) = \begin{cases} \sum_{i=1}^{2m-w} x_i + (w-m) \cdot y_i & w-m \geq 0 \\ R_{-(w-m)}(y, x) & w-m < 0 \end{cases} \quad (5)$$

Define the normalized cross-correlation coefficient ($NCCc$), and divide the mutual correlation sequence by the geometric mean of the respective sequence to make it translation-invariant. The maximum position of $NCCc$ is w . Obtain the SBD calculation as shown in Equation (6). The SBD range is $[0, 2]$, then the smaller the value, the higher the curve similarity is.

$$SBD(x, y) = 1 - \max_w \left(\frac{CC_w(x, y)}{\sqrt{R_0(x, x) \cdot R_0(y, y)}} \right) \quad (6)$$

(2) Time-series shape extraction:

The K-Shape algorithm takes the calculation of the centroid as an optimization problem, such that the centroid can represent the characteristics of the cluster; its objective

function is to obtain the cluster center μ_j^* corresponding to the maximum squared similarity with all other time series, as shown in Equation (7):

$$\mu_j^* = \operatorname{argmax}_{\mu_j} \sum_{x \in C_j} [NCC_c(x, \mu_j)]^2 \quad (7)$$

where C_j is the j th cluster; μ_j is the initial centroid of the j th cluster.

(3) Shape-based time series clustering:

This is achieved by randomly allocating time series data samples to multiple initial centers, calculating the centroids of each cluster, and using the *SBD* to measure the similarity of the time series. Repeat the above steps until the objective function converges, and finally, allocate the time series to different clusters and the centroids of each cluster (which represents the characteristics of the cluster, i.e., the centroids represent the typical features of the cluster).

The K-Shape algorithm can effectively cluster data samples with different “shapes”, but it can only be used for equal-“length” data samples and cannot analyze data with different “lengths”.

4.2.3. DDTW+K-Means++ Algorithm

In response to the problem of unequal time series length and unnatural data alignment in driving workload, the dynamic time warping (DTW) algorithm was used to calculate the optimal nonlinear alignment of the two time series [36]. For the time series $x = (x_1, \dots, x_m)$ and $y = (y_1, \dots, y_n)$, an $m \times n$ matrix M was constructed, where the term (i, j) is the Euclidean distance w_k of the time series data points x_i and y_j , and the continuous set containing the corresponding matching relationship of all points in the two time series is warping path $W = w_1, w_2, \dots, w_k$. The DTW algorithm can obtain the cumulative shortest path, as shown in Equation (8):

$$DTW(x, y) = \frac{1}{K_0} \sqrt{\sum_{i=1}^{K_0} w_i} \quad (8)$$

where K_0 is the length of the warping path, and to eliminate the impact of the different lengths of warping paths, this should be divided by K_0 . The corresponding relationship between two unequal-length time series data can be obtained by solving the recursive equation shown in Equation (9) through dynamic programming:

$$\gamma(i, j) = ED(x_i, y_j) + \min\{\gamma(i-1, j-1), \gamma(i-1, j), \gamma(i, j-1)\} \quad (9)$$

where $\gamma(i, j)$ is the total distance of the warping path accumulated up to row i and column j of the distance matrix.

In practical calculations, in order to find the shortest path, one point in one sequence often corresponds to multiple points in another sequence, resulting in the phenomenon of “Singularities”. In order to avoid the “Singularities” phenomenon, the Euclidean distance between two points is converted into the square of the difference of two point derivatives by calculating the derivatives of the time series data, which is called the derivative DTW (DDTW) algorithm. The derivative $D_x[x]$ estimation method is shown in Equation (10) [37]:

$$D_x[x] = \frac{(x_i - x_{i-1}) + [(x_{i+1} - x_{i-1})/2]}{2} \quad 1 < i < m \quad (10)$$

After obtaining the optimal nonlinear alignment of the time series by using the DDTW algorithm, it can be combined with a conventional unsupervised clustering algorithm to cluster the tunnel length. To avoid errors in clustering results caused by the unreasonable selection of the initial center of the cluster in the K-Means algorithm, use the K-Means++ algorithm [38,39]. Firstly, randomly select a data sample as the initial center of the first cluster. Next, the initial centers of the other clusters are determined by calculation with the

initial center of the first cluster. The data sample with the largest distance is selected as the initial center of the other clusters with a probability, i.e., the farther the distance, the higher the probability of it becoming the initial center is. By conducting this, the discreteness of the K clusters can be ensured, and the effectiveness of the clustering can be improved.

On the basis of data normalization, this paper selected the DDTW algorithm to process the time series with different lengths of the average driving workload in tunnels, and it used the K-Means algorithm to cluster the tunnel length. The K-Means algorithm and the K-Shape algorithm (which interpolated the time series) were also used for the comparative analysis of the clustering results. According to the subjective driving experience of the participants, the tunnel should be classified into 3 or 4 categories; thus, the number of clusters $K = 2, 3, 4,$ and 5 was taken for calculation.

4.3. Clustering Results

To evaluate the quality of the clustering results and to determine the number of clusters, $d(x_i, x_j)$ was defined as the distance between two vectors x_i, x_j , and $d(x_i, X_i)$ was defined as the distance between vector x_i and cluster X_i . Furthermore, $d(x_i, \mu_i)$ was defined as the distance of vector x_i from cluster center μ_i of cluster X_i , and $d(\mu_i, \mu_j)$ was defined as the distance between cluster centers μ_i, μ_j . The following internal evaluation indexes were used to analyze the clustering results:

- (1) Sum of squared error (SSE):

The SSE is the Euclidean distance from the data sample to the cluster center of the cluster, as shown in Equation (11):

$$SSE = \sum_{i=1}^K \sum_{x \in X_i} d^2(x, \mu_i) \quad (11)$$

- (2) Davies–Bouldin index (DBI):

The DBI is the ratio of the sum of the average distances within the cluster to the distance of the cluster center, as shown in Equation (12):

$$DBI = \frac{1}{K} \sum_{i=1}^K \max_{i \neq j} \left\{ \frac{d(x_i, X_i) + d(x_j, X_j)}{d(\mu_i, \mu_j)} \right\} \quad (12)$$

- (3) Compactness (CP):

CP is the average value of the distance between the data in the cluster and the cluster center, as shown in Equation (13):

$$CP = \frac{1}{K} \sum_{i=1}^K \frac{1}{|X_i|} \sum_{x_i \in X_i} d(x_i, \mu_i)^2 \quad (13)$$

- (4) Separation (SP):

SP is the average value of the cluster center distance between different clusters, as shown in Equation (14):

$$SP = \frac{2}{K(K-1)} \sum_{i=1}^K \sum_{j=i+1}^K d(\mu_i, \mu_j)^2 \quad (14)$$

Among them, the smaller the values of the SSE, DBI, and CP and the larger the values of SP, the better the clustering effect is. The comparison of the clustering results' evaluation indicators for each algorithm is shown in Table 3.

Table 3. Comparison of the clustering results of various algorithms.

K Algorithm	2			3			4			5		
	A	B	C	A	B	C	A	B	C	A	B	C
SSE	0.0098	0.0080	0.0076	0.0062	0.0052	0.0048	0.0058	0.0045	0.0042	0.0054	0.0038	0.0039
DBI	0.0102	0.0088	0.0084	0.0075	0.0056	0.0051	0.0062	0.0040	0.0041	0.0055	0.0041	0.0038
CP	0.0287	0.0198	0.0174	0.0187	0.0117	0.0101	0.0141	0.0099	0.0091	0.0124	0.0093	0.0084
SP	0.0245	0.0541	0.0654	0.0412	0.0765	0.0861	0.0346	0.0614	0.0645	0.0274	0.0511	0.0587

A is DDTW+K-Means++ algorithm; B is K-Shape algorithm; C is K-Means algorithm.

The results indicated that the DDTW+K-Means++ algorithm used in the paper outperformed the K-means algorithm in terms of all indicators, where its average accuracy was about 52.8% higher in comparison. Compared to the K-Shape algorithm, the DDTW+K-Means++ algorithm performed better for most indicators; only a few indicators were slightly worse, and this was when the number of clusters was high due to the sample number limitation; the overall average accuracy was about 8.3% higher.

The SSE, DBI, and CP represent the distance within the cluster, which gradually decreases with the increase in the number of clusters. As shown in Figure 3, when $K = 3$, the decrease in the values of the SSE, DBI, and CP slowed down significantly; when $K = 4$ and 5, the growth of the clustering accuracy obtained by increasing the number of clusters decreased. SP represents the distance between clusters, and when $K = 3$, the value of SP was the highest. This indicated that $K = 3$ was the optimal number of clusters.

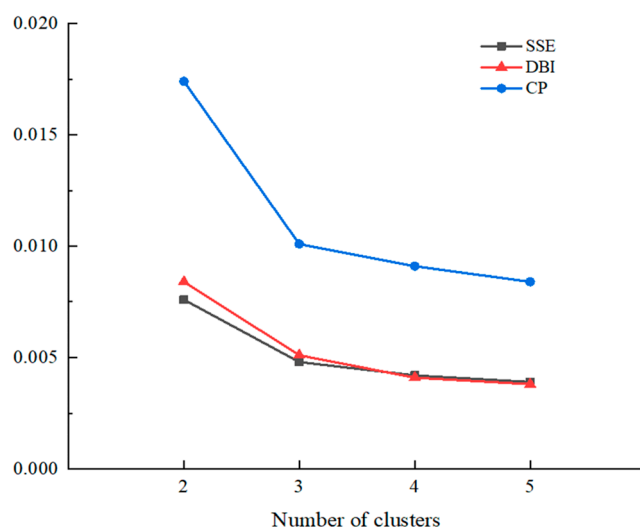


Figure 3. Comparison of the SSE, DBI, and CP indicators in the clustering results of the DDTW+K-Means++ algorithm.

Therefore, the results at $K = 3$ under the DDTW+K-Means++ algorithm were chosen to effectively characterize, based on the driving workload, the classification of tunnels of different lengths.

When $K = 3$, the DDTW+K-Means++ algorithm clustered the tunnels into three categories by length. The clustering results and typical tunnels (which were processed by DDTW) are shown in Figure 4.

- (1) Category 1: tunnel length of 54~466 m. A tunnel with a length of 450 m or less is defined as a short tunnel.
- (2) Category 2: tunnel length of 444~3962 m. A tunnel with a length of 450~4000 m is defined as a general tunnel.
- (3) Category 3: tunnel length of 4352~12,330 m. A tunnel with a length of 4000 m or more is defined as a long tunnel.

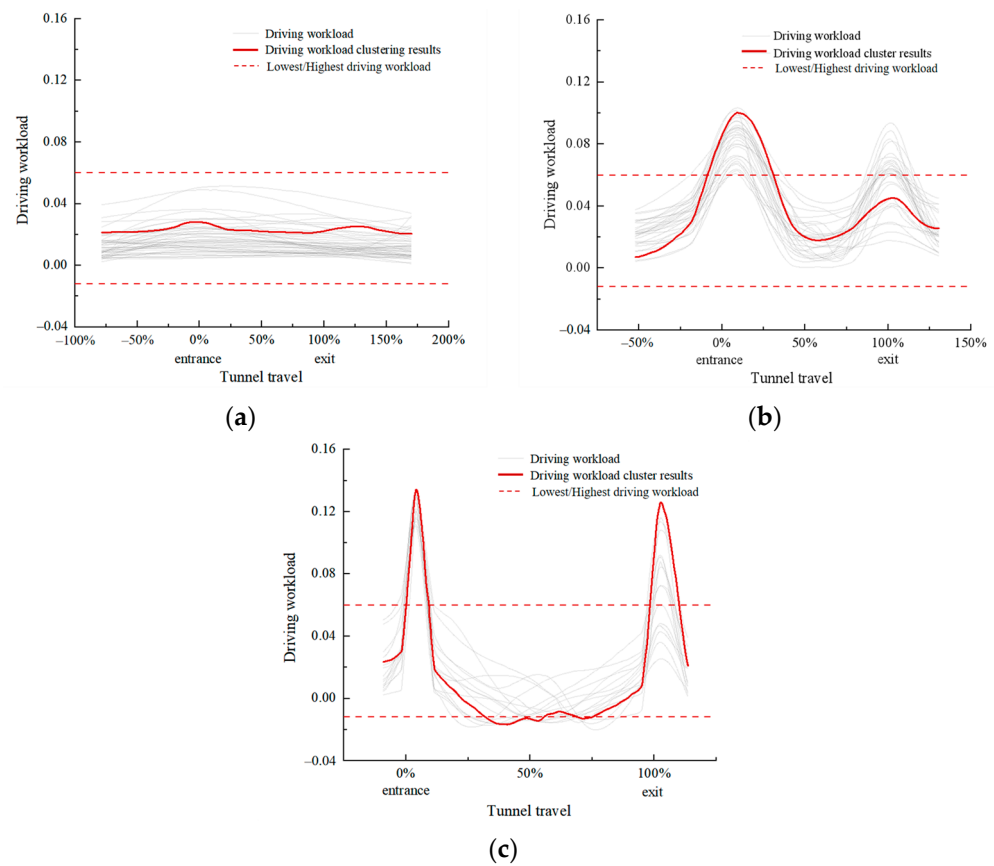


Figure 4. Clustering results and typical tunnels (353 m, 1612 m, and 8262 m). (a) Category 1 clustering results (typical tunnel 353 m); (b) Category 2 clustering results (typical tunnel 1612 m); (c) Category 3 clustering results (typical tunnel 8262 m).

5. Cluster Analysis of Tunnel Length

The vehicle speeds and driving workload for different locations (short tunnels without a middle area) in the three categories of the tunnels in the experiment were collated, as shown in Tables 4 and 5.

Table 4. Results of the vehicle speed statistics for different categories of tunnels.

Tunnel	Site	Maximum Speed (km/h)	Minimum Speed (km/h)	Running Speed (km/h)	Mean Speed (km/h)	SD	Speed Limit Compliance Rate
/	S	102.54	66.01	96.94	88.13	10.28	23.61%
Short Tunnel	A	95.86	59.95	86.98	80.04	10.09	45.52%
	B	83.68	49.61	74.44	64.40	9.79	90.63%
	D	90.80	60.58	85.25	74.31	9.78	63.85%
	E	96.54	63.06	86.82	78.29	9.90	51.02%
General Tunnel	A	95.80	58.05	84.89	76.83	10.40	62.57%
	B	81.65	48.43	70.89	61.82	9.36	93.86%
	C	86.93	60.67	77.97	73.87	6.59	90.31%
	D	87.14	53.42	73.76	65.50	8.98	86.74%
	E	91.54	56.94	82.86	74.10	10.72	67.58%
Long Tunnel	A	94.77	56.55	84.88	76.65	10.84	65.87%
	B	82.65	46.43	69.01	60.86	9.03	95.88%
	C	92.26	56.10	82.90	75.10	10.93	73.28%
	D	86.29	50.66	69.93	64.10	8.77	93.75%
	E	89.22	52.16	82.30	72.65	10.95	70.51%

Table 5. Results of the driving workload statistics for different categories of tunnels.

Tunnel	Site	Maximum	Minimum	Mean	SD	Higher Risk Ratio	High Risk Ratio
/	S	0.03541	−0.00412	0.00614	0.00701	2.01%	0.00%
Short Tunnel	A	0.04957	0.00205	0.01631	0.00940	8.05%	0.00%
	B	0.05125	0.00445	0.01825	0.01035	11.02%	0.00%
	D	0.05254	0.00513	0.01635	0.00939	10.06%	0.00%
	E	0.04445	0.00079	0.01387	0.00783	4.55%	0.00%
General Tunnel	A	0.05857	0.00412	0.02509	0.00901	28.51%	0.00%
	B	0.10306	0.00211	0.05760	0.02126	89.72%	46.27%
	C	0.05162	0.00021	0.01841	0.00981	11.73%	0.00%
	D	0.09316	0.00008	0.04677	0.01796	78.82%	25.37%
	E	0.05786	0.00756	0.02967	0.01036	44.09%	0.00%
Long Tunnel	A	0.06384	0.00244	0.02467	0.01535	30.98%	2.36%
	B	0.13396	0.00487	0.07944	0.03304	91.68%	69.41%
	C	0.05886	−0.02064	0.00220	0.01470	51.72%	21.20%
	D	0.12596	−0.00932	0.05834	0.03022	80.77%	45.48%
	E	0.07778	0.00124	0.03136	0.01695	47.62%	6.88%

A total of 15 sets of vehicle speed data were used. The S-W normality test results for a standard freeway section and for the different sites of the three categories of tunnels were 0.053~0.547 > 0.05, which are in accordance with a normal distribution. At the same time, the driving workload was a Log-normal distribution.

There was a significant difference in the average vehicle speed and driving workload between the standard freeway section and the three categories of tunnels at the 95% confidence level based on a U-test. When the participants were on the standard freeway section (S), the road conditions were good and the vehicle speed was fast. In addition, the speed limit compliance rate was low (23.61%), and the speed dispersion was large; at the same time, the driving task was simple; the driving workload was normal, and only a few participants experienced slight driving fatigue. After crossing through the standard freeway section (S), 100~200 m before the tunnel information sign, the participants clearly recognized the tunnel information sign and drove into the tunnel preview area (A). The affected area of the tunnel started to produce different degrees of stimulation of the participants, and different categories of tunnels had different impacts on the participants' driving behaviors and driving workload.

5.1. Short Tunnel

The vehicle speed of the short tunnels is shown in Figure 5a; the driving workload of the short tunnels is shown in Figure 5b; the changes in vehicle speed and driving workload in a typical short tunnel (353 m) are shown in Figure 5c.

There was no tunnel preview sign in the short tunnel, and the participants' recognition of the tunnel information signs in the preview area (A) saw their driving workload rise slightly. In addition, the participants began to be affected by the tunnel and began to reduce their speed; but the vehicle speed was still high. After entering the entrance area (B), the participants felt the change in road conditions such as at the cross-section; thus, the driving workload further increased; the vehicle running speed (74.44 km/h) decreased significantly; the majority of participants (90.63%) complied with the speed limit. The short tunnels were mostly non-optical long tunnels that were without the "black hole" and "white hole" phenomena. The participants in the tunnel entrance that were before one stopping sight distance could completely see the tunnel exit and understood the tunnel conditions. As such, the driving workload of the second half of the entrance area (B) and the exit section (D) began to reduce; thus, the speed increased. After exiting the tunnel exit, the impact of the tunnel on the separation area (E) further decreased or even disappeared, and the driving workload and vehicle speed gradually changed to be consistent with the standard

freeway section (S). The short tunnel affected area had less of an impact on the participants as their overall driving workload was normal and due to only a few of these tunnels having higher-risk sections.

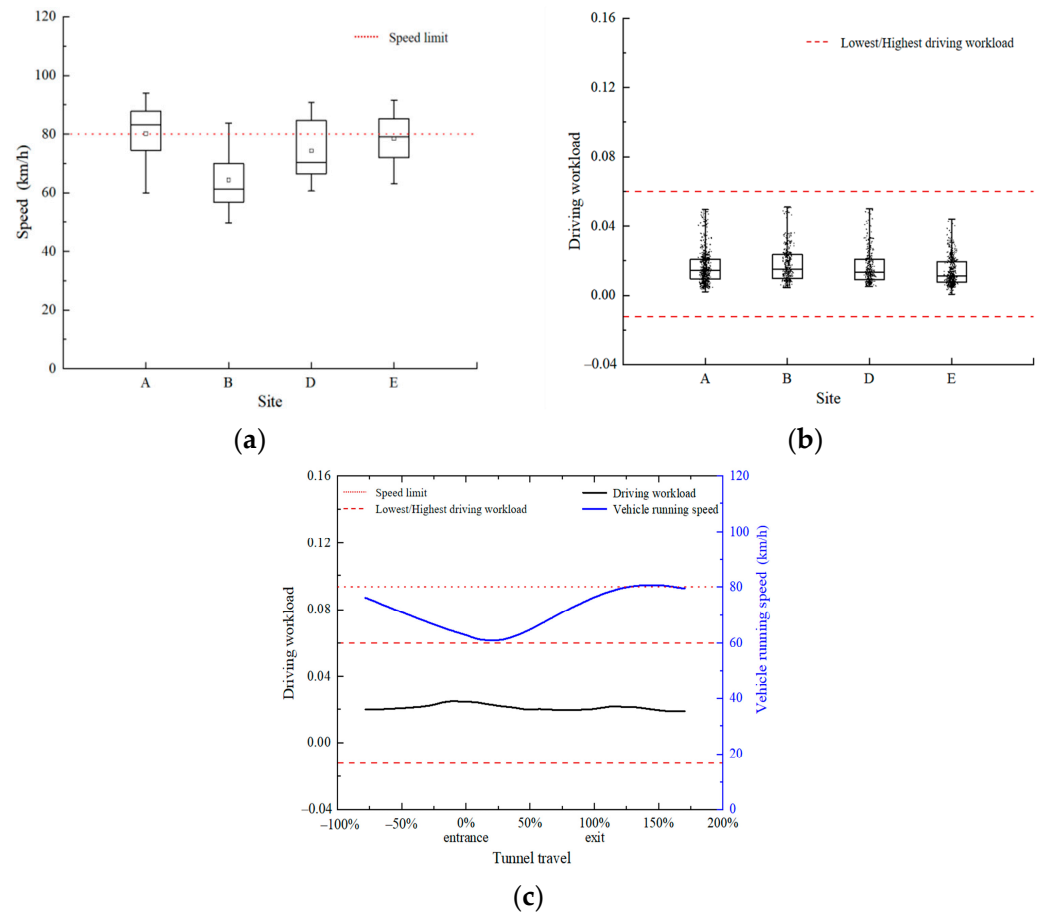


Figure 5. Vehicle speed and driving workload in the short tunnels. (a) Distribution of vehicle speed for short tunnels; (b) distribution of driving workload for short tunnels; (c) changes in vehicle speed and driving workload in a typical short tunnel (353 m).

5.2. General Tunnel

The vehicle speed of the general tunnels is shown in Figure 6a; the driving workload of the general tunnels is shown in Figure 6b; the changes in vehicle speed and driving workload in a typical general tunnel (1612 m) are shown in Figure 6c.

Most of the general tunnels were equipped with tunnel preview signs before the tunnel information signs. The participants were informed of the tunnel part with the information before the preview area (A), and the vehicle running speed was relatively smooth. Similar to the short tunnels, in the preview area (A), the participants started to be affected by the tunnel, and their vehicle speed decreased; however, the road conditions had not yet changed in the preview area (A), and the participants had different driving styles, thus resulting in greater vehicle speed dispersion. The entrance area's (B) road and lighting environment changed suddenly, and there was the "black hole" and "white hole" phenomena, thus leading to a significant increase in the driving workload and a significant decrease in the vehicle speed. As the participants gradually adapted to the tunnel environment, the driving workload decreased to a normal level. As lane changing was not allowed in the tunnel, the driving task was simple, and the vehicle speed in the middle area (C) rose, while the participants traveled steadily, whereby the vehicle running speed (77.97 km/h) was not significantly different from the speed limit and the speed dispersion (6.59) was low. With an accumulation of driving travel, when the participants

saw the tunnel exit, they developed a sense of escape and began to accelerate out of the tunnel. Furthermore, at that time, the lighting environment of the exit section (D) changed, and this had an impact on the participants as their driving workload rapidly increased and their vehicle speed decreased. The road conditions of the separation area (E) returned to normal; thus, the driving workload and vehicle speed gradually returned to normal. Compared to short tunnels, the general tunnels had significant changes in their road and environmental conditions, resulting in significant fluctuations in the driving workload at the different sites; they also presented increased safety risks, and a certain proportion of them had high-risk sections at the tunnel entrances and exits.

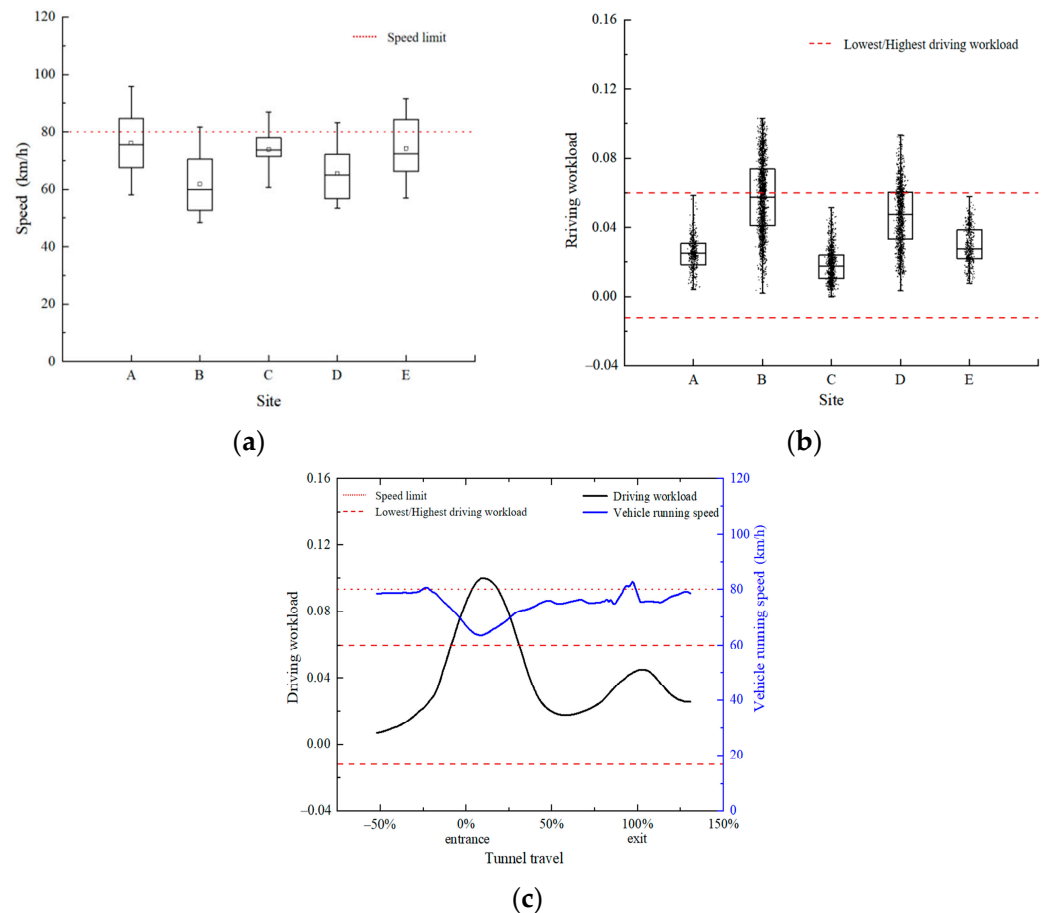


Figure 6. Vehicle speed and driving workload in the general tunnels. (a) Distribution of vehicle speed for general tunnels; (b) distribution of driving workload for general tunnels; (c) changes in vehicle speed and driving workload in a typical general tunnel (1612 m).

5.3. Long Tunnel

The vehicle speed of the long tunnels is shown in Figure 7a; the driving workload of the long tunnels is shown in Figure 7b; the changes in vehicle speed and driving workload in a typical long tunnel (8262 m) are shown in Figure 7c.

The long tunnels exhibited the same trend as the general tunnels in their preview area (A) and entrance area (B), but the long tunnels had a more-significant impact on the participants, with a higher driving workload and lower vehicle speeds. After driving in the middle area (C) for a period of time, the participants were affected by the monotonous environment in the tunnel and by having a single driving task. The participants began to show different degrees of driving fatigue as their driving workload was significantly reduced. Certain participants appeared to unconsciously accelerate, and the vehicle running speed (82.90 km/h) and speed dispersion (10.93) increased compared to the same in the general tunnels. However, the participants then adjusted themselves; the driving workload

increased and fluctuated above and below the fatigue threshold, thus resulting in a decrease in the vehicle speed. The exit area (D) and separation area (E) were similar to the same in the general tunnels, but the long tunnels had, to a greater extent and for a longer period of time, a higher driving workload and impact on the participants. There were high-risk sections in the different sites of the long tunnels with a relatively high proportion of high-risk sections in the entrance area (B), middle area (C), and exit area (D). The high-risk sections in the entrance area (B) and exit area (D) were mainly caused by the high driving workload, while the middle area (C) was due to the low driving workload.

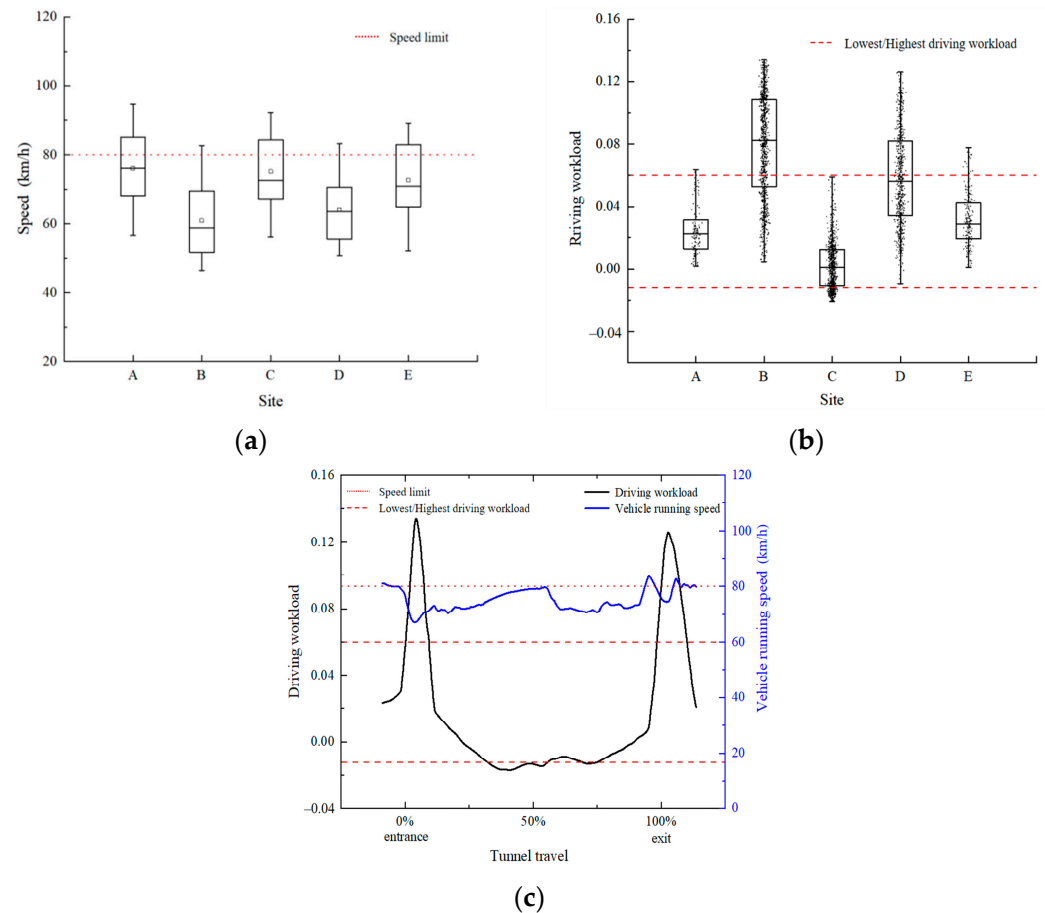


Figure 7. Vehicle speed and driving workload in the long tunnels. (a) Distribution of vehicle speed for long tunnels; (b) distribution of driving workload for long tunnels; (c) changes in vehicle speed and driving workload in a typical long tunnel (8262 m).

6. Discussion

In this work, the impact of the different lengths of the tunnels on the drivers' driving workload and driving behavior was studied through a naturalistic driving experiment. The DDTW+K-Means++ algorithm was used to cluster the tunnels into three categories based on the driving workload in line with the tunnel length. Tunnel classification is the foundation for tunnel operation safety management. Currently, different scholars and related specifications mainly classify tunnels into 3~6 categories based on civil and electromechanical design [26–29], with less consideration of tunnel operation safety management requirements. Too few tunnel classifications will lead to a reduction in the accuracy of traffic safety facility settings and operational safety management, thus increasing operational safety risks. Too many tunnel classifications will cause the management workload to rise and make it more difficult to manage. As road users, the subjective feelings and changes in the driving workload of drivers indicate that tunnels should be classified into three categories. It can be on the basis of ensuring the accuracy of operational safety management

that management can be carried out based on the subjective feelings of drivers, the driving workload, and the driving behavior, thus reducing management difficulty and ensuring tunnel operation safety.

Good road alignment conditions lead to higher vehicle running speeds, with varying degrees of speeding at all sites in the natural driving experiment. The participants kept driving at a high speed in the standard freeway section (S). After driving into the affected area of the tunnel, due to the preview area (A) road and environmental conditions having not yet changed, certain, more-aggressive, participants' driving workload was low, and they still maintained a high speed; when the more-conservative personality-type participants' driving workload rose, they reduced the speed of their driving. Thus, it can be seen that personality preferences led to an increase in speed dispersion. The rapid changes in road and environmental conditions at the entrance area and exit area led to a steep increase in the participants' driving workload. In addition, there was a significant reduction in vehicle speed, thus resulting in an uncoordinated running speed in the adjacent sections. An increase in tunnel length will exacerbate this phenomenon. The difference in the vehicle running speed between the entrance area (B) and standard freeway section (S) of the different categories of tunnels was greater than 20 km/h, and the difference between the preview area (A) and the entrance area (B) was greater than 10 km/h. The increase in the vehicle running speed, the speed difference between adjacent sections, and the speed dispersion will lead to the decrease in traffic safety [40]. Thus, undertaking a reasonable speed limit strategy could reduce the safety risk in the affected area of the tunnel [41]. Therefore, in tunnel design and in operational safety management, the drivers' driving workload and driving behavior characteristics under different tunnel categories and sites should be fully considered; in addition, appropriate speed limit strategies and methods should be adopted to reduce the operational safety risks in the affected area of the tunnel.

Studies related to tunnel safety have indicated that the entrance area is the highest-risk site of the tunnel in terms of affecting regional operational safety, and its accident pattern is mainly rear-end accidents—accounting for more than 2/3 of all accidents [42]. Short tunnels have better visibility; their visual perception changes earlier than is the case in normal and long tunnels [25], with a lower driving workload and lower operational safety risks. General tunnels and long tunnels generally induce the “black hole” and “white hole” phenomena, which will, thus, lead to a sharp increase in the driving workload, the speed, deceleration, gaze point, and sweeping amplitude being significantly different, and inducing a high risk of operation safety when compared to short tunnels. Vision is the main way through which drivers obtain road and traffic information, with visual acquisition accounting for over 80% of all information. The uncomfortable transition of the lighting environment at the entrance area and exit area leads to the reduction in the driver's visual recognition efficiency, or it can even induce the phenomenon of “blind vision”. Coupled with changes in road cross-sections, the driving workload increases, resulting in the entrance area and exit area and the adjacent section of the vehicle running speed not being coordinated; the entrance area speed dispersion is too large, and it is the main cause of accidents. Long tunnels have more-drastring changes in the lighting environment compared to general tunnels, resulting in greater operation safety risks. Therefore, for general tunnels and long tunnels, the lighting environment design should be improved, along with the use of variable color temperature intelligent lighting technology; these measures will help to protect the safety of the entrance area and exit area.

The driving environment in the middle area of a long tunnel is monotonous and closed; it is also influenced by the linear shape, traffic volume, and lighting environment conditions. When a driver is driving in the middle area of a long tunnel for a long time, the driver's brain receives less stimulation, and the amount of thinking, judgment, and operation is small; this will lead to slow reactions, weakened perceptions, a reduced level of consciousness, reduced alertness, psychological depression, and gradually produce driving fatigue. In the experiment, drivers in the middle area of all the long tunnels had different degrees of driving fatigue, and driving fatigue is also an important feature that

distinguishes long tunnels from short tunnels and general tunnels. Relevant research has indicated that, when the vehicle running speed is 60~100 km/h in the tunnel, drivers will experience different levels of driving fatigue at different sites in the middle area of the tunnel [43]. With involuntary acceleration, increased speed dispersion, and even sleep, the traffic safety risk will increase sharply. A fatigue arousal section with blue, purple, and cyan lights should be set on the side walls of the tunnel to give drivers stimulation, such that they can return to a normal driving condition. At the same time, further research should be conducted on the setting location, length, brightness, and other setting techniques for the fatigue arousal sections of different tunnels.

This paper only selected freeway tunnels with a design speed limit of 80 km/h for the experiment. When the design speed and restricted speed are 60 km/h or 100 km/h, the length of each category of the tunnels will change. When the road conditions remained unchanged, there was a positive correlation between the driving workload and vehicle running speed. A low driving workload and low volatility at lower speeds resulted in shorter lengths of each category of tunnel. A high driving workload and high volatility at higher speeds, which take longer for drivers to return to normal driving workload, resulted in longer lengths of each category of tunnel. When the vehicle running speed was higher, the driving workload grew faster and the length of each category of tunnels grew faster, i.e., the length of each category of tunnels did not have a linear relationship with the vehicle running speed, which can be analyzed in a focused manner in future studies.

7. Conclusions

This paper conducted a clustering study on tunnels of different lengths in freeways via a naturalistic driving experiment. The impact of the different categories of tunnels on the drivers' driving safety, comfort driving workload, and driving behavior were analyzed. The following conclusions were drawn:

1. The driving workload and vehicle speed characteristics of the 98 freeway tunnels of different lengths were obtained based on a naturalistic driving experiment involving 36 participants. The DDTW+K-means++ algorithm was used to cluster the tunnel lengths based on tunnel driving workload time series data. The results indicated that, in the tunnel operation stage, it is reasonable to divide tunnels into three categories according to their length (i.e., short tunnels were <450 m, general tunnels were 450~4000 m, and long tunnels were >4000 m).
2. There were significant differences in the driving workload and vehicle running speed between the different categories of tunnels; the length of the tunnel had a positive correlation with the driving workload, while there was a negative correlation with the vehicle running speed. The range of changes in the driving workload and operation safety risks in the general tunnels and long tunnels were higher than those in the short tunnels.
3. There were significant differences in the driving workload and vehicle running speed between the different sites in the tunnels. The road and environmental conditions were also important factors that affected the driving workload. The entrance area and exit area were the sections where the driving workload changed sharply and where the vehicle running speed was reduced, thus resulting in the adjacent sections of the vehicle running speed not being coordinated. Furthermore, the speed dispersion was large, thus increasing the risk of operational safety. Lastly, the driving workload in the middle area of the long tunnels was low; thus, there was more driving fatigue.

The research results of this paper can provide a basis for a more-refined management of freeway tunnel operation safety, which is of great significance in reducing the accident rate and accident severity in tunnels and can be utilized to guarantee tunnel safety. In this work, only the design speed and vehicle running speed of 80 km/h freeway tunnels were studied. The traffic, road, the environment on the coupling effect of the driving workload, and the classification of tunnels at different speeds need further research and demonstration.

Author Contributions: Conceptualization, J.H. and S.M.; methodology, J.H. and S.M.; validation, E.M. and W.L.; formal analysis, S.M. and R.W.; investigation, E.M. and W.L.; resources, E.M. and W.L.; data curation, J.H. and S.M.; writing—original draft preparation, S.M.; writing—review and editing, J.H. and R.W.; visualization, S.M.; supervision, J.H. All authors have read and agreed to the published version of the manuscript.

Funding: This research was funded by the key field research and development plan projects of Department of Science and Technology of Guangdong Province (No. 2022B0101070001).

Institutional Review Board Statement: Not applicable.

Informed Consent Statement: Not applicable.

Data Availability Statement: The data generated in this study are available upon request.

Acknowledgments: The authors would like to thank all the participants in the experiments.

Conflicts of Interest: The authors declare no conflict of interest.

Nomenclatures

Nomenclature	Meaning	Unit
A_i	HRV when driver i is driving normally	/
$CC_w(x,y)$	A mutual correlation sequence of length $2m^{-1}$	/
C_i	Set containing samples in category i	/
C_j	j th cluster	/
$dist(C_i, x_i)$	Distance between C_i and x_i	/
$d(x_i, X_i)$	Distance between vector x_i and cluster X_i	/
$d(x_i, x_j)$	Distance between two vectors x_i, x_j	/
$d(x_i, \mu_i)$	Distance of vector x_i from cluster center μ_i of cluster X_i	/
$d(\mu_i, \mu_j)$	Distance between cluster centers μ_i, μ_j	/
$D_x[x]$	Derivative	/
ED	Euclidean distance	/
HF	High-frequency power	/
(i,j)	Euclidean distance w_k of the time series data points x_i and y_j	/
k	Traffic volume	veh/km·ln
K	Number of categories	/
K_0	Length of the warping path	/
K_{ij}	Driving workload of driver i at position j	/
LF	Low-frequency power	/
$(LF/HF)_{ij}$	HRV of driver i at position j	/
M	$m \times n$ matrix	/
$NCCc$	Normalized cross-correlation coefficient	/
R	Sum of the dot products of the effective regions	/
SBD	Shape-based distance	/
V_{ij}	Running speed when driver i is at position j	km/h
w	Maximum position of NCCc	/
W	Warping path	/
$x = (x_1, \dots, x_m)$	Time series x	/
$y = (y_1, \dots, y_m)$	Time series y	/
$\gamma(i,j)$	Total distance of the warping path accumulated up to row i and column j of the distance matrix	/
μ_j^*	Initial centroid of the j th cluster	/
μ_j	Cluster center corresponding to the maximum squared similarity with all other time series	/

Abbreviations

Abbreviations	Meaning
CP	Compactness
DBI	Davies–Bouldin index
DDTW	Derivative dynamic time warping
DTW	Dynamic time warping
GPS	Global Positioning System
HR	Heart rate
HRG	Heart rate growth
HRV	Heart rate variability
M	Mean value
SD	Standard deviation
SP	Separation
SSE	Sum of squared error

References

- Du, Z.; Wang, S.; Yang, L.; Ni, Y.; Jiao, F. Experimental study on the efficacy of retroreflective rings in the curved freeways tunnels. *Tunn. Undergr. Space Technol.* **2021**, *110*, 103813. [[CrossRef](#)]
- Wang, X.; Wen, R.; Cheng, K.; Yang, M. Evaluation and analysis of tunnel lighting service status based on driving safety. *Traffic Inj. Prev.* **2023**, *24*, 436–444. [[CrossRef](#)]
- Wang, K.; Hu, J.; Chen, R.; Wang, J. A study on the evacuation of an extra-long highway tunnel fire—A case study of Chengkai Tunnel. *Sustainability* **2023**, *15*, 4865. [[CrossRef](#)]
- Amundsen, F.H.; Ranæs, G. Studies on traffic accidents in Norwegian road tunnels. *Tunn. Undergr. Space Technol.* **2000**, *15*, 3–11. [[CrossRef](#)]
- Ma, Z.; Shao, C.; Zhang, S. Characteristics of traffic accidents in Chinese freeway tunnels. *Tunn. Undergr. Space Technol.* **2009**, *24*, 350–355. [[CrossRef](#)]
- Yang, Y.; Chen, Y.; Wu, C.; Easa, S.; Lin, W.; Zheng, X. Effect of highway directional signs on driver mental workload and behavior using eye movement and brain wave. *Accid. Anal. Prev.* **2020**, *146*, 105705. [[CrossRef](#)]
- Lee, J.; Kirytopoulos, K.; Pervez, A.; Huang, H. Understanding drivers' awareness, habits and intentions inside road tunnels for effective safety policies. *Accid. Anal. Prev.* **2022**, *172*, 106690. [[CrossRef](#)]
- Chen, J.; You, L.; Yang, M.; Wang, X. Traffic safety assessment and prediction under different lighting service states in road tunnels. *Tunn. Undergr. Space Technol.* **2023**, *134*, 105001. [[CrossRef](#)]
- Llopis, S.G. Traffic accidents in Spanish road tunnels. In *Proceedings of the Institution of Civil Engineers-Transport*; Thomas Telford Ltd.: London, UK, 2018; Volume 175, pp. 43–49. [[CrossRef](#)]
- Pena-García, A. Sustainable tunnel lighting: One decade of proposals, advances and open points. *Tunn. Undergr. Space Technol.* **2021**, *119*, 104227. [[CrossRef](#)]
- Jiao, F.; Du, Z.; Zheng, H.; Wang, S.; Han, L.; Chen, C. Visual characteristics of drivers at different sections of an urban underpass tunnel entrance: An experimental study. *Sustainability* **2021**, *13*, 5224. [[CrossRef](#)]
- Sun, H.; Wang, Q.; Zhang, P.; Zhong, Y.; Yue, X. Spatiotemporal characteristics of tunnel traffic accidents in China from 2001 to Present. *Adv. Civ. Eng.* **2019**, *2019*, 4536414. [[CrossRef](#)]
- Xu, X.; Kang, X.; Wang, X.; Zhao, X.; Si, C. Research on spiral tunnel exit speed prediction model based on driver characteristics. *Sustainability* **2022**, *14*, 15736. [[CrossRef](#)]
- Kirytopoulos, K.; Kazaras, K.; Papapavlou, P.; Ntzeremes, P.; Tatsiopoulos, I. Exploring driving habits and safety critical behavioural intentions among road tunnel users: A questionnaire survey in Greece. *Tunn. Undergr. Space Technol.* **2017**, *63*, 244–251. [[CrossRef](#)]
- Wen, H.; Sun, J.; Zeng, Q.; Zhang, X.; Yuan, Q. The effects of traffic composition on freeway crash frequency by injury severity: A bayesian multivariate spatial modeling approach. *J. Adv. Transport.* **2018**, *2018*, 6964828. [[CrossRef](#)]
- Calvi, A.; De Blasiis, M.R.; Guattari, C. An empirical study of the effects of road tunnel on driving performance. *Procedia Soc. Behav. Sci.* **2012**, *53*, 1098–1108. [[CrossRef](#)]
- Calvi, A.; Amico, F.D. A study of the effects of road tunnel on driver behavior and road safety using driving simulator. *Adv. Transp. Stud.* **2013**, *30*, 57–76.
- Wang, S.; Du, Z.; Jiao, F.; Zheng, H.; Ni, Y. Drivers' visual load at different time periods in entrance and exit zones of extra-long tunnel. *Traffic Inj. Prev.* **2020**, *21*, 539–544. [[CrossRef](#)]
- Feng, Z.; Yang, M.; Zhang, W.; Du, Y.; Bai, H. Effect of longitudinal slope of urban underpass tunnels on drivers' heart rate and speed: A study based on a real vehicle experiment. *Tunn. Undergr. Space Technol.* **2018**, *81*, 525–533. [[CrossRef](#)]
- Yang, Y.; Du, Z.; Jiao, F.; Pan, F. Analysis of EEG characteristics of drivers and driving safety in undersea tunnel. *Int. J. Environ. Res. Public Health* **2021**, *18*, 9810. [[CrossRef](#)]

21. Rendon-Velez, E.; van Leeuwen, P.M.; Happee, R.; Horváth, I.; van der Vegte, W.F.; de Winter, J.C.F. The effects of time pressure on driver performance and physiological activity: A driving simulator study. *Transp. Res. Part F Traffic Psychol. Behav.* **2016**, *41*, 150–169. [[CrossRef](#)]
22. Qi, W.; Shen, B.; Wang, L. Model of driver's eye movement and ECG index under tunnel environment based on spatiotemporal data. *J. Adv. Transport.* **2020**, *2020*, 5215479. [[CrossRef](#)]
23. Yang, Y.; Chen, J.; Easa, S.M.; Zheng, X.; Lin, W.; Peng, Y. Driving simulator study of the comparative effectiveness of monolingual and bilingual guide signs on Chinese highways. *Transport. Res. F-Traf.* **2020**, *68*, 67–78. [[CrossRef](#)]
24. Pawar, N.M.; Velaga, N.R.; Sharmila, R.B. Exploring behavioral validity of driving simulator under time pressure driving conditions of professional drivers. *Transp. Res. Part F Traffic Psychol. Behav.* **2022**, *89*, 67–78. [[CrossRef](#)]
25. Fu, X.; He, S.; Du, J.; Wang, X.; Ge, T. Variations in naturalistic driving behavior and visual perception at the entrances of short, medium, and long tunnels. *J. Adv. Transport.* **2020**, *2020*, 7630681. [[CrossRef](#)]
26. Mashimo, H. State of the road tunnel safety technology in Japan. *Tunn. Undergr. Space Technol.* **2002**, *17*, 145–152. [[CrossRef](#)]
27. British Standards Institution. *Code of Practice for the Design of Road Lighting-Part 2: Lighting of Tunnels*; BS 5489-2:2003+A1:2008; BSI Group Headquarters: London, UK, 2008.
28. Kim, H.K.; Loennermark, A.; Ingason, H. Comparison of road tunnel design guidelines. In Proceedings of the Third International Symposium on Tunnel Safety and Security, Stockholm, Sweden, 12–14 March 2008.
29. Ministry of Transport of the People's Republic of China. *Specifications for Design of Highway Tunnels-Section 1 Civil Engineering*; JTG 3370.1-2018; China Communications Press: Beijing, China, 2019.
30. Chen, X.; Guo, X. Research on Classification Methods for Operational Management of Highway Tunnels. *Technol. Highw. Transp.* **2010**, *90*, 121–123+128.
31. Ma, S.; Hu, J.; Wang, R.; Qu, S. Study on the median opening length of a freeway work zone based on a naturalistic driving experiment. *Appl. Sci.* **2023**, *13*, 851. [[CrossRef](#)]
32. Wei, W.; Fu, X.; Zhong, S.; Ge, H. Driver's mental workload classification using physiological, traffic flow and environmental factors. *Transp. Res. Part F Traffic Psychol. Behav.* **2023**, *94*, 151–169. [[CrossRef](#)]
33. Choi, K.-H.; Kim, J.; Kwon, O.S.; Kim, M.J.; Ryu, Y.H.; Park, J.-E. Is heart rate variability (HRV) an adequate tool for evaluating human emotions?—A focus on the use of the International Affective Picture System (IAPS). *Psychiat. Res.* **2017**, *251*, 192–196. [[CrossRef](#)]
34. Wang, C.; Chan, Y.; Chu, S.; Yu, S. *r*-Reference points based *k*-means algorithm. *Inform. Sci.* **2022**, *610*, 204–214. [[CrossRef](#)]
35. Paparrizos, J.; Gravano, L. *k*-Shape: Efficient and accurate clustering of time series. *Sigmod. Rec.* **2016**, *45*, 69–76. [[CrossRef](#)]
36. Rakthanmanon, T.; Campana, B.; Mueen, A.; Batista, G.; Westover, B.; Zhu, Q.; Zakaria, J.; Keogh, E. Searching and mining trillions of time series subsequences under dynamic time warping. In Proceedings of the 18th ACM SIGKDD International Conference on Knowledge Discovery and Data Mining—KDD' 12, Beijing, China, 12–16 August 2012.
37. Keogh, E.J.; Pazzani, M.J. Derivative dynamic time warping. In Proceedings of the 2001 SIAM international Conference on Data Mining, Chicago, IL, USA, 5–7 April 2001.
38. Baldassi, C. Recombinator-*k*-Means: An evolutionary algorithm that exploits *k*-Means plus plus for recombination. *IEEE Trans. Evol. Comput.* **2022**, *26*, 991–1003. [[CrossRef](#)]
39. Meng, J.; Yu, Z.; Cai, Y.; Wang, X. *K*-Means++ clustering algorithm in categorization of glass cultural relics. *Appl. Sci.* **2023**, *13*, 4736. [[CrossRef](#)]
40. Lee, Y.M.; Chong, S.Y.; Goonting, K.; Sheppard, E. The effect of speed limit credibility on drivers' speed choice. *Transp. Res. Part F Traffic Psychol. Behav.* **2017**, *45*, 43–53. [[CrossRef](#)]
41. Jung, S.; Qin, X. Data-Driven approach to weather-responsive speed management of road tunnel access zones. *Transport. Res. Rec.* **2022**, *2676*, 1–12. [[CrossRef](#)]
42. Meng, Q.; Qu, X. Estimation of rear-end vehicle crash frequencies in urban road tunnels. *Accident Anal. Prev.* **2012**, *48*, 254–263. [[CrossRef](#)]
43. Qin, P.; Wang, M.; Chen, Z.; Yan, G.; Yan, T.; Han, C.; Bao, Y.; Wang, X. Characteristics of driver fatigue and fatigue-relieving effect of special light belt in extra-long highway tunnel: A real-road driving study. *Tunn. Undergr. Space Technol.* **2021**, *114*, 103990. [[CrossRef](#)]

Disclaimer/Publisher's Note: The statements, opinions and data contained in all publications are solely those of the individual author(s) and contributor(s) and not of MDPI and/or the editor(s). MDPI and/or the editor(s) disclaim responsibility for any injury to people or property resulting from any ideas, methods, instructions or products referred to in the content.